STEM CELLS TRANSLATIONAL MEDICINE®

TISSUE ENGINEERING AND REGENERATIVE MEDICINE

Defining the Optimal Window for Cranial Transplantation of Human Induced Pluripotent Stem Cell-Derived Cells to Ameliorate Radiation-Induced Cognitive Impairment

MUNJAL M. ACHARYA,[a] VAHAN MARTIROSIAN,[a] LORI-ANN CHRISTIE,[a] LARA RIPARIP,[a] JAN STRNADEL,[b] VIPAN K. PARIHAR,[a] CHARLES L. LIMOLI[a]

Key Words. Induced pluripotent stem cell-derived human neural stem cells • Transplantation • Radiation • Cognition • Hippocampus • Novel place recognition • Fear conditioning

[a]Department of Radiation Oncology, University of California, Irvine, Irvine, California, USA; [b]Department of Pathology, University of California, San Diego, La Jolla, California, USA

Correspondence: Charles L. Limoli, Ph.D., Department of Radiation Oncology, University of California, Irvine, Medical Sciences I, Room B-146B, Irvine, California 92697-2695, USA. Telephone: 949-824-3053; E-Mail: climoli@uci.edu

Received March 28, 2014; accepted for publication October 8, 2014; first published online in SCTM *EXPRESS* November 12, 2014.

1066-5099/2014/$20.00/0

http://dx.doi.org/10.5966/sctm.2014-0063

ABSTRACT

Past preclinical studies have demonstrated the capability of using human stem cell transplantation in the irradiated brain to ameliorate radiation-induced cognitive dysfunction. Intrahippocampal transplantation of human embryonic stem cells and human neural stem cells (hNSCs) was found to functionally restore cognition in rats 1 and 4 months after cranial irradiation. To optimize the potential therapeutic benefits of human stem cell transplantation, we have further defined optimal transplantation windows for maximizing cognitive benefits after irradiation and used induced pluripotent stem cell-derived hNSCs (iPSC-hNSCs) that may eventually help minimize graft rejection in the host brain. For these studies, animals given an acute head-only dose of 10 Gy were grafted with iPSC-hNSCs at 2 days, 2 weeks, or 4 weeks following irradiation. Animals receiving stem cell grafts showed improved hippocampal spatial memory and contextual fear-conditioning performance compared with irradiated sham-surgery controls when analyzed 1 month after transplantation surgery. Importantly, superior performance was evident when stem cell grafting was delayed by 4 weeks following irradiation compared with animals grafted at earlier times. Analysis of the 4-week cohort showed that the surviving grafted cells migrated throughout the CA1 and CA3 subfields of the host hippocampus and differentiated into neuronal (~39%) and astroglial (~14%) subtypes. Furthermore, radiation-induced inflammation was significantly attenuated across multiple hippocampal subfields in animals receiving iPSC-hNSCs at 4 weeks after irradiation. These studies expand our prior findings to demonstrate that protracted stem cell grafting provides improved cognitive benefits following irradiation that are associated with reduced neuroinflammation. STEM CELLS TRANSLATIONAL MEDICINE *2015;4:74–83*

INTRODUCTION

Although cranial radiotherapy is beneficial for the treatment of central nervous system (CNS) malignancies, it frequently leads to a wide variety of progressive and debilitating cognitive deficits [1, 2]. These serious side effects affect an increasing number of cancer survivors who are forced to endure persisting cognitive decrements that adversely affect quality of life with little or no clinical recourse for neurocognitive decline [3, 4]. Cognitive impairments found after cranial radiotherapy are multifaceted and manifest as impaired hippocampal-dependent (and independent) learning and memory, frequently including altered attention, concentration, and executive functions, such as planning and multitasking [2]. The mechanisms underlying radiation-induced cognitive dysfunction are incompletely understood; however, significant past data from our laboratory have shown the beneficial cognitive effects of human stem cell transplantation following cranial irradiation [5–7].

Intrahippocampal transplantation of human stem cells was used to explore possible interventions targeted against the long-term neurocognitive sequelae resulting from cytotoxic cancer therapies, including radiotherapy and chemotherapy. We have shown that radio- and chemotherapy regimens modeled to approximate clinical scenarios deplete sensitive populations of neural stem and progenitor cells, inhibit neurogenesis, induce neuroinflammation, and severely compromise neuronal structure [8–11]. In almost every instance, each of the foregoing sequelae is ameliorated to varying degrees by stem cell grafting, indicating that the varied beneficial effects of stem cell therapy are likely to be complex and involve multiple mechanisms.

The fact that ionizing radiation depletes radiosensitive mulitpotent stem cells in the brain prompted initial efforts to restore these populations by stem cell grafting following cranial

irradiation. Much of our past work using a variety of human stem cell types involved transplantation 2 days following irradiation [5–7]. Although these studies indicated the benefits of this strategy, related data in spinal cord injury [12] have shown that stem cell grafting is most beneficial when transplanted at delayed time following the initial insult. To better define the optimal transplantation window for maximizing the beneficial effects of stem cell grafting into the irradiated brain, we varied the postirradiation time of transplantation and normalized cognitive testing to 1 month following transplantation surgery. With this paradigm, we identified that delaying transplantation by 1 month provides the greatest cognitive benefits compared with shorter intervals between irradiation and stem cell grafting. We report the beneficial cognitive effects of transplanting induced pluripotent stem cell-derived (iPSC-derived) human neural stem cells (hNSCs) in the irradiated rodent brain and how the cells differentiate and mitigate neuroinflammation throughout multiple hippocampal subfields.

Materials and Methods

Animals and Irradiation

All animal procedures were approved based on institutional animal care and use committee and federal (NIH) guidelines. As in previous studies [5–7], an immunocompromised athymic nude (ATN) rat model (strain 0N01, Cr:NIH-rnu) was used for all experimentation. A total of 44 male ATN rats (2 months old; Frederick National Laboratory for Cancer Research, Frederick, MD, http://frederick.cancer.gov) were maintained in sterile housing conditions (20°C $\pm$ 1°C; 70% $\pm$ 10% humidity; 12 hours each light and dark cycle) and with ready access to sterilized diet and water.

Animals were divided into five groups: 0-Gy (no irradiation) sham-surgery controls (CON; n = 8), 10-Gy irradiated sham surgery (IRR; n = 12), and 10-Gy irradiated with iPSC-derived hNSCs (iPSC-hNSCs) engrafted at 2 days (IRR+iPSC$_{2d}$), 2 weeks (IRR+iPSC$_{2w}$), or 4 weeks (IRR+iPSC$_{4w}$) after irradiation (n = 8 per group). Anesthetized rats were shielded to protect the eyes and body and were subjected to cranial-only γ-irradiation (10 Gy) using a cesium 137 irradiator (Mark I; J.L. Shepard, San Fernando, CA, http://www.jlshepherd.com) at a dose rate of 2.07 Gy/minute, as described previously [6, 7].

Transplantation Surgery

The use of human stem cells was approved by the institutional human stem cell research oversight committee under a material transfer agreement with the University of California San Diego (UCSD). The iPSC-hNSCs originated from a normal skin biopsy, as described previously [13]. Their derivation and use were approved by UCSD institutional review board (approval identifier 100887). The iPSC-hNSCs were expanded and sorted for a CD184$^+$/CD24$^+$/CD44$^-$/CD271$^-$ fraction using a FACSAria sorter (BD Biosciences, San Diego, CA, http://www.bdbiosciences.com), as described previously [13]. The purified population of proliferating iPSC-hNSCs were maintained on EnStem-A neural expansion media (Millipore, Billerica, MA, http://www.millipore.com) containing neurobasal media supplemented with L-glutamine (2 mM; Invitrogen, Carlsbad, CA, http://www.invitrogen.com), basic fibroblast growth factor (20 ng/ml; Millipore), B27 and leukemia inhibitory factor (Millipore) and was routinely passaged (1:2) every other day. For transplantation, iPSC-hNSCs were used from passages 37–39, for which viability was routinely $\geq$90%. For transplantation of nonstem cells, human IMR-90 normal fibroblasts (Coriell Cell Repositories, Camden, NJ, https://catalog.coriell.org) were used between passages 8 and 11, maintained in Modified Eagle's Medium (MEM; Gibco, Grand Island, NY, http://www.invitrogen.com; Life Technologies, Rockville, MD, http://www.lifetech.com) supplemented with 10% fetal bovine serum (FBS; Gibco). Prior to transplantation surgery, fibroblasts were washed repeatedly with MEM to remove FBS.

A schematic of our experimental paradigm is shown in Figure 1. At the selected postirradiation transplantation time, each rat received bilateral intrahippocampal transplantation of 100,000 live iPSC-hNSCs (IRR+iPSC) in 1 μl of cell suspension using a 33-gauge microsyringe at an injection rate of 0.25 μl/minute. Each hippocampus received 4 distinct injections (total 4.0 $\times$ 10^5 live cells per hemisphere) using precise stereotaxic coordinates, as described previously [5–7]. Sham-surgery unirradiated controls and irradiated cohorts received sterile vehicle (hibernation buffer) at the same stereotaxic coordinates.

In a separate series of studies, a similar group of control and irradiated cohorts were used for comparisons with those transplanted with normal human fibroblasts (IMR-90) 2 days following cranial irradiation (IRR+IMR-90$_{2d}$).

Cognitive Testing

To evaluate the outcome of iPSC-derived hNSC transplantation on cognitive function, rats from each cohort (CON, IRR, and IRR+iPSC$_{2d,\ 2w,\ 4w}$) were tested on novel place recognition (NPR) and contextual and cued fear-conditioning (FC) tasks, as described previously [5, 7, 14]. For the CON and IRR cohorts, animals were subjected to cognitive testing 2 months after irradiation (to coincide with the IRR+iPS$_{4w}$ cohort), and data derived at this time were comparable to past data analyzing similar cohorts 1 month after irradiation [5, 7]. For animals receiving stem cells, all cognitive testing was initiated 1 month following transplantation surgery, such that only the time between irradiation and surgery was varied.

The NPR task provides an assessment of spatial recognition memory and relies on intact hippocampal function [5, 7, 14]. The FC task was administered in three sequential phases over 3 days, including a training phase, a context test, and a cue test. Although cued FC memory relies on intact amygdala function, the contextual version of FC memory also engages the hippocampus [14]. For all FC phases, rats were placed in a PhenoTyper 3000 (Noldus Information Technology, Leesburg, VA, http://www.noldus.com) equipped with a video camera for observation and live animal tracking during FC trials. All cohorts were tested on NPR followed by FC. For each task, video recording and automated tracking of the animals were carried out using a Noldus EthoVision XT system (v8.0; Noldus Information Technology). Detailed procedures for the NPR and FC tasks have been described previously [5, 7, 14].

Immunohistochemistry and Confocal Microscopy

Following cognitive testing, animals were sacrificed and perfused with 4% paraformaldehyde (Acros Organics, Geel, Belgium, http://www.acros.com), and brain tissues were processed for coronal sectioning (30-μm thick using a cryostat; Leica Microsystems, Wetzlar, Germany, http://www.leica.com). Immunohistochemical analyses of iPSC-hNSCs used both monoclonal and polyclonal antibodies. The following primary antibodies were used: anti-Ku80 (Stem101, human specific DNA telomere-binding

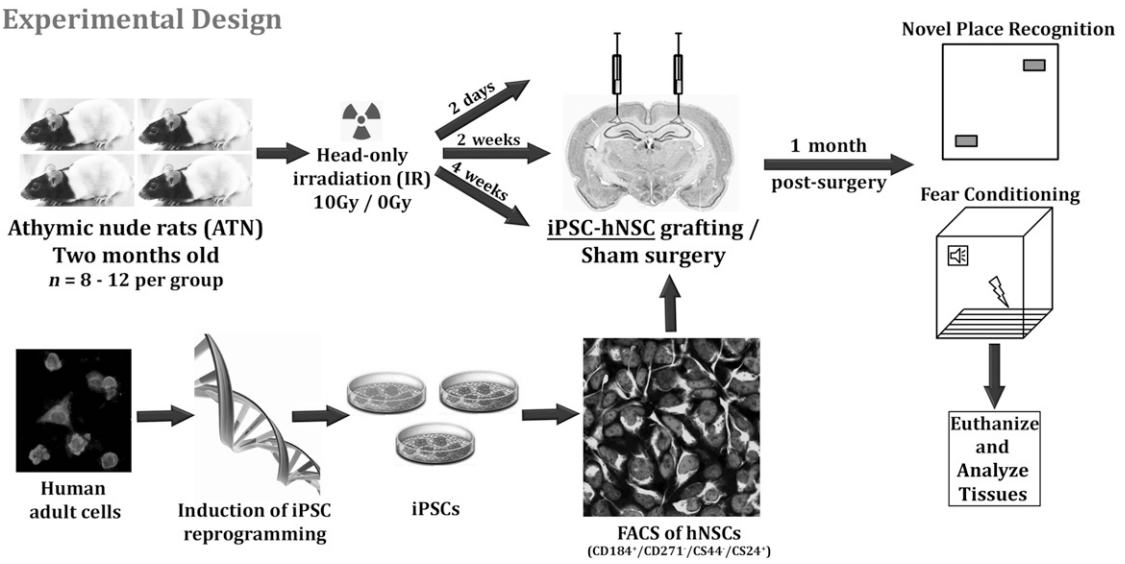

Figure 1. Schematic of experimental design. Two-month-old athymic nude rats received 10-Gy head-only γ-irradiation and were divided into three groups for iPSC-derived human neural stem cell transplantation: 2 days, 2 weeks, and 4 weeks after irradiation. At 1 month following transplantation surgery, animals were administered a novel place recognition task and a fear conditioning task. After completion of cognitive testing, animals were euthanized for immunohistochemical analyses. Nonirradiated control (0 Gy) and irradiated (10 Gy) animals receiving sterile cell culture media served as sham surgery groups. Abbreviations: FACS, fluorescence-activated cell sorting; hNSC, human neural stem cell; iPSC, induced pluripotent stem cell.

nuclear protein, mouse, 1:100; StemCells Inc., Cambridge, U.K., http://www.stemcellsinc.com), anti-DCX (doublecortin, goat; Santa Cruz Biotechnology Inc., Santa Cruz, CA, http://www.scbt.com), anti-Tuj1 (βIII-tubulin, rabbit, 1:200; Covance, Princeton, NJ, http://www.covance.com), anti-NeuN (neuron-specific nuclear antigen, rabbit, 1:250; EMD Millipore, Billerica, MA, http://www.millipore.com), anti-GFAP (glial fibrillary acidic protein, rabbit, 1:500; EMD Millipore), anti-S100 (S100β protein, rabbit, 1:200; EMD Millipore), anti-nestin and Ki-67 (rabbit, 1:200; EMD Millipore), anti-NG2 (oligoprogenitor marker, chondroitin sulfate proteoglycan 4, rabbit; EMD Millipore), anti-O4 (mature oligodendrocytes, mouse monoclonal; R&D Systems Inc., Minneapolis, MN, http://www.rndsystems.com), anti-ED-1 (CD68, activated microglia, mouse monoclonal; AbD Serotec, Raleigh, NC, http://www.ab-direct.com). The secondary antibodies and detection reagents included biotinylated horse anti-goat IgG (1:200; Vector Laboratories, Burlingame, CA, http://www.vectorlabs.com), donkey anti-mouse and anti-rabbit conjugated with Alexa Fluor 488 or 594 (1:200; Life Technologies, Invitrogen) and TOTO-3 iodide (infrared nuclear counterstain; Life Technologies, Invitrogen).

To determine the differentiated fate of transplanted iPSC-derived hNSCs, representative sections through transplantation sites were stained using a free-floating dual-immunofluorescence technique for human-specific nuclear antigen (Ku80) and various mature and immature neuronal (DCX, Tuj1, NeuN), astrocytic (GFAP, S100), oligodendroglial (NG2, O4), and cycling (Ki-67, nestin) markers, as described previously [5, 7]. Serial sections taken through the middle of the hippocampus were selected for staining and stored in Tris-buffered saline (TBS; 100 mM, pH 7.4; Sigma-Aldrich, St. Louis, MO, http://www.sigmaaldrich.com) overnight. Free-floating sections were first rinsed in TBS followed by Tris-A (TBS with 0.1% Triton-X-100; Sigma-Aldrich), blocked with 10% normal donkey serum (NDS with Tris-A; Sigma-Aldrich) and incubated overnight in a mouse anti-Ku80 antibody (1:100) prepared in 3% NDS and Tris-A. The next day, the sections were treated for 1 hour with donkey anti-mouse IgG Alexa Fluor 594 (1:200) made with Tris-A and 3% NDS. The sections were light protected, washed with Tris-A, and blocked in serum and primary antibodies for the other markers. Color development was facilitated by Alexa Fluor conjugated secondary antibodies, as described above, and counterstained with TOTO-3 nuclear dye (1 μmol/l in TBS, 15 minutes; Life Technologies, Invitrogen) for visualization of hippocampal morphology. Immunostained sections were rinsed in TBS and mounted on clean Vectabond-coated (Vector Laboratories) slides using SlowFade antifade mounting medium (Life Technologies, Invitrogen). Ku80$^+$ cells were visualized under fluorescence as red, and differentiation markers were visualized as green. For quantification of differentiated phenotypes, dual-labeled sections from representative hippocampal sections were analyzed from distinct transplants derived from four animals in each group. For the detection of engrafted human fibroblasts, similar procedures were followed using brains sections stained for human antigen-specific antibodies (anti-NuMA, 1:200; Cell Signaling Technology, Beverly, MA, http://www.cellsignal.com; anti-Ku80, 1:100; StemCells Inc.; anti-CD90, 1:200; Abcam, Cambridge, U.K., http://www.abcam.com).

To identify activated microglia (ED-1$^+$ cells), serial sections were washed with phosphate-buffered saline (PBS), blocked with 10% NDS in PBS containing 0.1% Triton X-100 (Sigma-Aldrich) for 30 minutes, and incubated overnight in primary ED-1 antibody prepared in PBS containing 2% NDS and 0.1% Triton X-100. On the second day, sections were washed and incubated for 1 hour in secondary antibody (donkey anti-mouse IgG, Alexa Fluor 594; Life Technologies, Invitrogen). Sections were then washed thoroughly and counterstained with nuclear dye TOTO-3 iodide (1 μmol/l in TBS for 15 minutes; Life Technologies, Invitrogen) to visualize the different hippocampal cell layers.

For the assessment of activated microglia (ED1+) in the hippocampus, every 15th section through the entire hippocampus (n = 3 animals each group) was subjected to stereological assessment using a Zeiss microscope (Carl Zeiss Microscopy, Jena, Germany,

http://www.zeiss.com) equipped with an MBF monochrome digital camera (MBF Biosciences, Williston, VT, http://www.mbfbioscience.com), ×100 (oil-immersion, 1.30 NA; Zeiss) objective lens, 3-axis motorized stage, and an optical fractionator probe (StereoInvestigator, MBF Biosciences). Separate contours were drawn for each hippocampal subfield (DH, GCL, CA3, and CA1). Systematic random sampling (SRS) and image stack analysis modules were used to acquire batch images that were uploaded to an MBF Biosciences workstation. The number of activated microglia was quantified by counting ED1-positive cells using the optical fractionator probe and SRS according to unbiased stereological principles. Sampling parameters (grid and counting frame size) were empirically determined to achieve low coefficients of error (<0.1) for each hippocampus. To identify the phenotypic fate of graft-derived cells, laser-scanning confocal analyses were performed using a Nikon Eclipse microscope (TE2000-U, EZ-C1 interface) equipped with red, green, and infrared lasers, as described previously [3, 4]. *z*-Stack analyses (1-μm intervals) and orthogonal image reconstruction were done using Nikon Elements AR software (v3.22; Nikon, Tokyo, Japan, http://www.nikon.com).

Statistical Analyses

Statistical analyses were carried out using PASW Statistics 18 (SPSS; IBM Corp., Armonk, NY, http://www-01.ibm.com/software/analytics/spss/). All analyses were two-tailed and considered a value of $p \leq .05$ to be statistically significant. In all data sets, normal distribution of the data (Kolmogorov-Smirnov test) and homogeneity of variance (Levene's test of equality of error variances) were confirmed. When overall group effects were found to be statistically significant, multiple comparisons were made using Fisher's protected least significant difference (FPLSD) post hoc tests to compare the individual groups.

For the NPR task, the exploration ratio—the proportion of total time spent exploring the novel spatial location ($t_{novel}/t_{novel} + t_{familiar}$)—was used as the main dependent measure. The behavior of the animals during the first minute of the 5-minute test phase was analyzed [5, 7, 14]. All animals in each cohort were included in the NPR task analyses.

For the FC task, the percentage of time spent freezing was used as the main dependent measure. Freezing was assessed during the final minute of the baseline (i.e., before tone-shock pairings were administered) and post-training (i.e., after tone-shock pairings) phases. For the context test, freezing was assessed over the entire 5-minute trial. For the precue test, freezing was assessed during the first minute (in the absence of tone); for the cue test, freezing was assessed over the 3-minute interval (in the presence of tone) and for the final minute of the trial (in the absence of tone). Repeated measures analysis of variance (ANOVA) was used to assess group (between-subjects factor) and phase (within-subjects factor) effects on freezing behavior [5, 14]. All animal cohorts subjected to NPR testing were subsequently analyzed for the FC task analyses.

RESULTS

Transplanted iPSC-Derived hNSCs Improve Cognition

Novel Place Recognition Task

One month after transplantation, animals were habituated and tested on the NPR task (Fig. 2A). Analysis of total time spent exploring both objects during the initial familiarization phase revealed an overall group difference ($p < .0001$, post hoc) (data not shown). Following a 5-minute retention interval, IRR animals spent a significantly lower proportion of time exploring the novel place compared with CON and all IRR+iPSC grafted cohorts

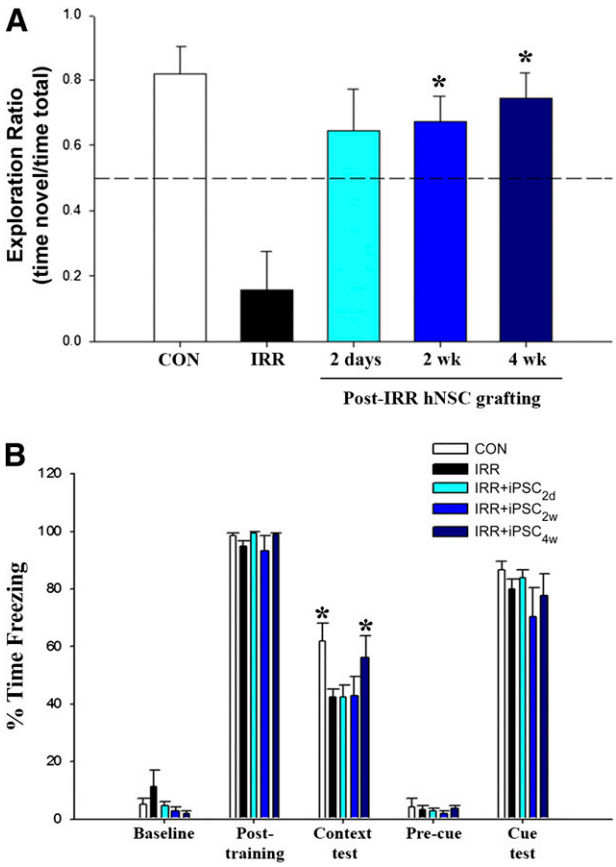

Figure 2. Human iPSC-derived neural stem cell transplantation ameliorated radiation-induced cognitive impairments. **(A):** For the novel place recognition (NPR) task, animals were habituated and familiarized with two identical objects in specific spatial locations in an open field arena, and total time spent exploring both identical objects was assessed. Following a 5-minute retention interval, animals were placed in the same arena with one object moved to a novel spatial location. Exploration ratios were calculated [$Time_{novel}$ / ($Time_{novel}$ + $Time_{familiar}$)] for the first minute of the NPR test session. IRR animals spent a significantly lower proportion of time exploring the novel place ($p < .001$ vs. CON and vs. iPSC-$hNSC_{2w\ \&\ 4w}$, post hoc), whereas CON and all IRR+iPSC animals did not differ. IRR animals did not spent more time exploring the novel place than expected by chance (dashed line at 50%). **(B):** For the context and cued fear-conditioning task, baseline freezing levels were established using a series of five tone-shock pairings (post-training bars), and all groups showed increased freezing behavior after training. At 24 hours later, a context test was administered, and the IRR and grafted cohorts (IRR+$iPSC_{2d}$ and IRR+$iPSC_{2w}$) spent significantly decreased percentages of time freezing compared with the CON group ($p = .05$), whereas CON and IRR+$iPSC_{4w}$ animals did not differ (context text bars). At 48 hours after the initial training phase, the context was changed, which resulted in a substantial reduction in freezing behavior in all groups (before cue bars). Furthermore, freezing levels were restored in all groups following the tone sound (cue test bars), indicating intact amygdala function in all groups. Data are presented as means +1 SEM. The *p* values were derived from Fisher's protected least significant difference post hoc comparisons. ∗, significant difference versus IRR animals. Abbreviations: 2d, 2-day group; 2w, 2-week group; 4w, 4-week group; CON, control; hNSC, human neural stem cell; iPSC, induced pluripotent stem cell; IRR, 10-Gy irradiated.

(all $p < .001$) (Fig. 2A). Furthermore, after the 5-minute retention interval, IRR+iPSC grafted animals did not differ from CON animals, whereas a trend indicated improved exploration for animals grafted at later times following irradiation. Moreover, one-sample *t* tests comparing the exploration ratios of individual groups with chance (0.5) (Fig. 2A, dashed line) revealed that CON, IRR+iPSC$_{2w}$, and IRR-iPSC$_{4w}$ animals spent significantly more time (all $p < .001$) exploring the novel place than expected by chance, whereas IRR animals explored the novel spatial location less than expected by chance.

Fear-Conditioning Task

The three phases of the FC task (training, cue, and context tests) were administered over 3 days. A significant overall group *x* phase interaction effect ($p = .049$) was found by repeated measures ANOVA for the percentage of time spent freezing during the FC task (Fig. 2B). Subsequent individual one-way ANOVAs conducted for each phase of the task revealed a significant group effect ($p = .031$) for the context test phase of the FC task (Fig. 2B, context test bars). Post hoc FPLSD tests showed that IRR animals and grafted cohorts IRR-iPSC$_{2d}$ and IRR-iPSC$_{2w}$ spent significantly decreased percentages of time freezing compared with the CON group ($p = .05$), whereas CON and IRR+iPSC$_{4w}$ cohorts did not differ. No significant group difference was observed in freezing behavior across baseline, post-training, precue test, and cue test phases (Fig. 2B), suggesting that irradiation induced a deficit selective for hippocampal-dependent contextual memory phase of the task. Irradiation was not found to impair motor or sensory function because all groups demonstrated significant increases in freezing behavior after the tone-shock pairings (post-training phase) (Fig. 2B). Furthermore, the fact that cued memory was intact demonstrates that the acquisition of the tone-shock pairing was not impaired and that the deficit was specific to the memory of the context in which the pairing was learned.

In a separate experiment, three cohorts (CON, IRR, and IRR+IMR-90$_{2d}$) of animals ($n = 8$ per group) were subjected to the FC task, as described above, to determine the potential efficacy of normal human fibroblasts in ameliorating radiation-induced cognitive decrements 1 month after surgery. Although significant group differences between post-training, context, and cue test phases of the FC task were found (ANOVA), both irradiated cohorts (IRR, IRR+IMR-90$_{2d}$) were found to spend significantly less time freezing compared with controls (supplemental online Fig. 1), indicating that the fibroblast used under these condition did not provide any beneficial neurocognitive effects.

Location of Surviving Grafted iPSC-Derived hNSCs in the Irradiated Rat Hippocampus

Following cognitive testing, animals ($n = 8$) from the IRR-iPSC$_{4w}$ group were euthanized for immunohistochemical analysis of surviving grafted cells (IRR-iPSC$_{4w}$ group only) or for neuroinflammation. The majority of the grafted human cells were located ventral to the CA1 subfield and just dorsal to the dentate gyrus (Fig. 3). Examination of the Ku80 (human-specific nuclear antigen, green) immunofluorescence against the TOTO-3 counterstained sections from the IRR+iPSC$_{4w}$ group revealed the presence of grafted cells along the entire septotemporal axis of the hippocampus (Fig. 3A). Visualization of the Ku80 marker (green) showed that transplanted cells remained in clusters close to the transplantation site, with few Ku80$^+$ cells found to migrate away from the transplant core in the irradiated host hippocampus (Fig. 3B, 3C). Furthermore, the location of the transplant did not overtly distort the host hippocampal cytoarchitecture (pink, TOTO-3 nuclear counterstain) (Fig. 3A) because stereotaxic coordinates were selected to minimize disturbance of the hippocampal milieu. At 1 month after surgery, evidence of engrafted human fibroblasts was not found because extensive marker analysis was unable to detect the presence of any surviving fibroblasts proximal or distal to transplantation sites (data not shown).

Differentiation of Transplanted iPSC-Derived hNSCs

To determine the phenotypic fate of grafted cells from the IRR+iPSC$_{4w}$ group, dual immunofluorescence and confocal *z*-stack analyses were carried out in representative sections of the IRR+iPSC$_{4w}$ group. Examination of dual immunofluorescence-stained Ku80$^+$ cells revealed that very few coexpress proliferative markers (Ki-67) (Fig. 4A) or multipotent markers (nestin) (Fig. 4B). These data suggested that the majority of grafted cells underwent differentiation, and analysis of double-labeled cells indicated that multiple immature and mature neuronal, astrocytic, and oligodendroglial phenotypes were present in the irradiated host hippocampus (Fig. 4). Transplant-derived cells were found to express immature neural markers (DCX$^+$, Tuj1$^+$) (Fig. 4C, 4D) and mature neuronal markers (NeuN$^+$) (Fig. 4E). Analysis of astrocytic differentiation revealed the presence of double-labeled immature astrocytes (GFAP$^+$) (Fig. 4F) and mature astrocytes (S100$^+$) (Fig. 4G) and double-labeled immature oligodendrocytes (NG2$^+$) (Fig. 4H) and mature oligodendrocytes (O4$^+$) (Fig. 4I). Orthogonal reconstructions of confocal *z*-stacks are shown for each marker (Fig. 4A–4I).

Quantification of Differentiated Cell Types Derived From Transplanted iPSC-Derived hNSCs

Quantification of differentiated phenotypes revealed that the majority of graft-derived cells expressed the immature neuronal markers doublecortin (DCX, 18.52% $\pm$ 6.2%) and βIII-tubulin (Tuj1, 18.9% $\pm$ 1.87%), with a smaller percentage showing expression of the mature neuronal marker NeuN (1.9% $\pm$ 0.60%) (Fig. 4J). The fraction of grafted cells committed to astrocytic fates was much smaller because the percentages of GFAP$^+$ (2.3% $\pm$ 0.80%) and S100β^+ (4.2% $\pm$ 0.90%) cells were much lower compared with neuronal fates (Fig. 4J). Similarly, the number of graft-derived cells expressing the oligodendrocyte markers NG2 (5.4% $\pm$ 1.08%) and O4 (1.7% $\pm$ 0.6%) were low in comparison with neuronal yields. Very few grafted cells expressed the proliferative marker Ki-67 (1.2% $\pm$ 0.6%) and the multipotent marker nestin (1.2% $\pm$ 0.70%) (Fig. 4J).

When the foregoing phenotypes are grouped (Fig. 4K), the preference of iPSC-derived hNSCs to adopt neuronal as opposed to astroglial fates becomes evident. Although nearly 40% of Ku80$^+$ cells express neuronal markers, only 6.4% and 7.1% expressed markers for astrocytes or oligodendrocytes, respectively. The fraction of cycling cells (Ki-67$^+$ and nestin$^+$) were found to be minimal (2.4%), indicating that, following iPSC-derived hNSC transplantation, the irradiated microenvironment of the brain promoted differentiation over proliferation.

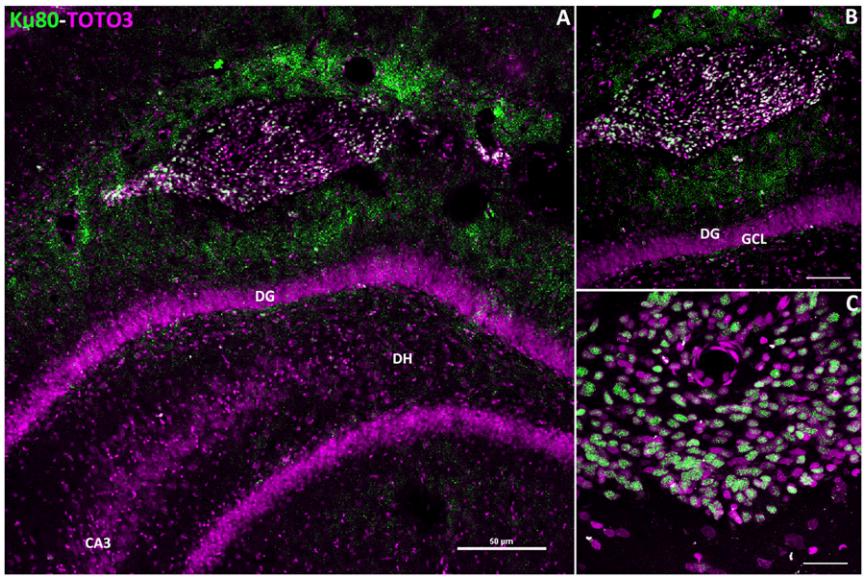

Figure 3. Survival and location of transplanted induced pluripotent stem cell-derived human neural stem cells (iPSC-hNSCs). At ~1.5 months after transplantation, graft-derived human cells (green) were located lateral to the CA1 subfield and extended near the CA3 subfield (**A–C**). Transplanted iPSC-hNSCs (green) did not show extensive migration into the DG or DH regions. Transplanted iPSC-hNSCs were detected by human-specific nuclear antigen (Ku80, green) and counterstained with nuclear dye (TOTO-3, pink). Scale bars: 50 μm **(A, B)**; 10 μm **(C)**. Abbreviations: DG, dentate gyrus; DH, dentate hilus; GCL, granule cell layer.

Microglial Activation Following Irradiation and Transplantation of iPSC-Derived hNSCs

Quantitative analyses of activated microglia (ED1+) using unbiased stererology revealed the presence of positive cells in all three cohorts analyzed (CON, IRR, and IRR+iPS4w) (Fig. 5A–5C). For the nongrafted cohorts (CON and IRR), all animals were sacrificed in parallel with the IRR+iPS4w group, such that the total time after irradiation was constant (i.e., 2.5 months) for the quantitative assessment of activated microglia. Irradiation triggered a significant ($p < .05$) increase in the number of ED1+ cells in the hiipocampus (Fig. 5D). Activated microglia increased by 4–5-fold compared with controls in each of the hippocampal subfields analyzed (dentate hilus [DH], granule cell layer [GCL], and CA3+CA1; Fig. 5D). Importantly, the increased numbers of activated microglia in each of the irradiated hippocampal subfields were significantly ($p < .05$) reduced by stem cell transplantation (Fig. 5D, 5E). The yield of activated microglia was not found to differ between controls and grafted cohorts (Fig. 5D, 5E). These data clearly suggest that iPS-derived hNSC transplantation significantly attenuated neuroinflammation in the irradiated brain.

Discussion

The unintended side effects associated with the radiotherapy of brain tumors include progressive and debilitating cognitive impairments that adversely affect quality of life. Although these serious problems have been recognized for years, there remains little clinical recourse for alleviating these persistent symptoms in patients surviving various cancer therapies. Much of our past work has characterized certain beneficial effects of human stem cell-based therapies for treating radiation-induced cognitive dysfunction, and the current study has further defined the transplantation window for optimizing the beneficial cognitive effects of grafted human stem cells. For much of our prior work [5–7], cranial transplantation of stem cells occurred over relatively brief times (i.e., 2 days) following irradiation. New findings reported in this paper point to the advantages of protracting the interval between irradiation and transplantation.

In the present work, we also chose to investigate the potential utility of using iPSC-derived hNSCs for ameliorating the adverse effects of irradiation on the brain. Despite certain caveats associated with the genetic stability and mutational spectrum of iPSCs derived from somatic cells [15, 16], their potential to provide multipotent progeny that minimize immunorejection under autologous and/or allogeneic transplant scenarios still holds considerable practical, if not theoretical, appeal. Rats receiving head-only irradiation and stem cell grafting were found to exhibit improved performance, as assessed by two well-characterized and widely used cognitive tasks (Fig. 2). The use of iPSC-derived hNSCs was found to elicit significant improvements on the NPR task at 1 month following each of the different postirradiation transplantation times, with a trend showing optimal performance with increased intervals between irradiation and transplantation (Fig. 2A). As opposed to the irradiated cohort, the performance of animals receiving irradiation and grafts (i.e., IRR+iPSC$_{2d,\ 2w,\ 4w}$) was indistinguishable from sham-surgery controls (Fig. 2A), with both controls and transplanted animals showing significant preference for exploring the novel place. Furthermore, exploration ratios found were comparable to those detailed in several of our past reports [5–7, 14].

To quantify further the effects of irradiation on cognition, we interrogated animals using a contextual fear-conditioning task that does not rely on spontaneous exploration but is still known to engage the hippocampus [17]. Animals subjected to cranial irradiation spent significantly less time engaged in freezing behavior than controls during the context phase of the task and were indistinguishable from irradiated animals grafted 2 days

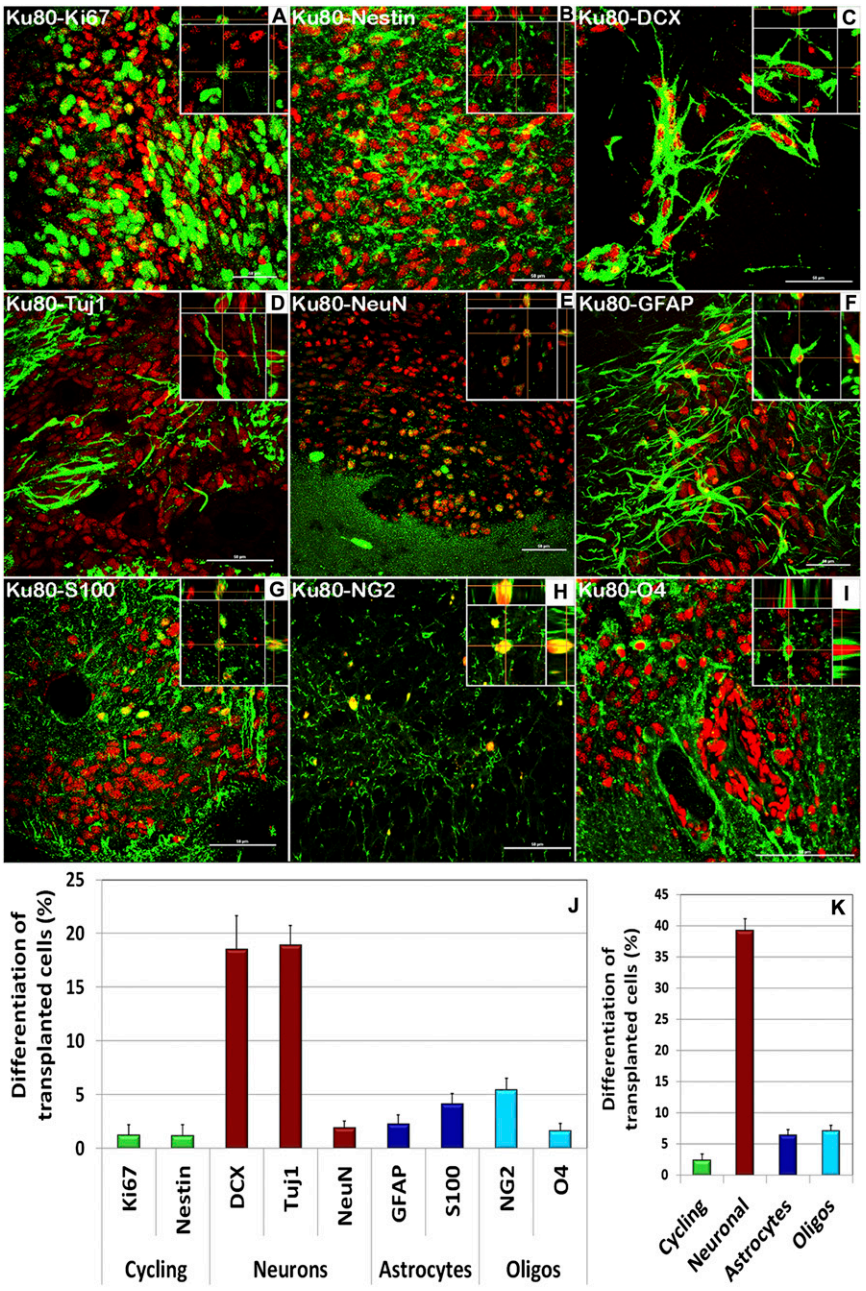

Figure 4. Differentiation of transplanted induced pluripotent stem cell-derived human neural stem cells (iPSC-hNSCs) in the irradiated hippocampus. Transplantation of iPSC-hNSCs at 4 weeks after irradiation yielded neuronal and astroglial phenotypes when analyzed at 1.5 months after surgery. Graft-derived IPSC-hNSCs (red, human nuclear antigen, $Ku80^+$) occasionally expressed cell cycle markers (green, Ki-67) **(A)** and multipotent markers (green, nestin) **(B)**. The majority of engrafted cells (green, $Ku80^+$) differentiated into immature neurons (green, double-cortin, DCX^+ and $Tuj1^+$) **(C, D)** and mature neurons (green, $NeuN^+$) **(E)**. A small fraction of graft-derived cells also expressed immature and mature astrocytes (green, GFAP and S100) **(F, G)** and oligodendroglial markers (green, NG2 and O4) **(H, I)**. For each panel, inserts represent orthogonal reconstructions of confocal *z*-stacks. The percentage of differentiated individual **(J)** and combined **(K)** phenotypes is shown. Scale bars: 50 μm **(A–I)**. Abbreviation: Oligos, oligodendrocytes.

or 2 weeks after irradiation (i.e., IRR+$iPSC_{2d,\ 2w}$) (Fig. 2B). These data suggest that irradiation disrupted 24-hour memory for the shock-context association, which has been shown to rely on intact hippocampal function [18], and that earlier grafting times were unable to impart cognitive benefits under these testing conditions (Fig. 2B). Interestingly, animals engrafted with iPSC-derived hNSCs at 4 weeks following irradiation (i.e., IRR+$iPSC_{4w}$) demonstrated intact freezing behavior and were statistically indistinguishable from controls in their contextual fear memory (Fig. 2B). This finding indicates that radiation-induced deficits in hippocampal function could be ameliorated when transplantation of stem cells is delayed by 1 month after irradiation. The amount of post-training freezing observed was comparable among all experimental cohorts, suggesting that irradiation, sham surgery, and/or transplantation of stem cells did not affect initial acquisition of the conditioned freezing response. Similarly, the

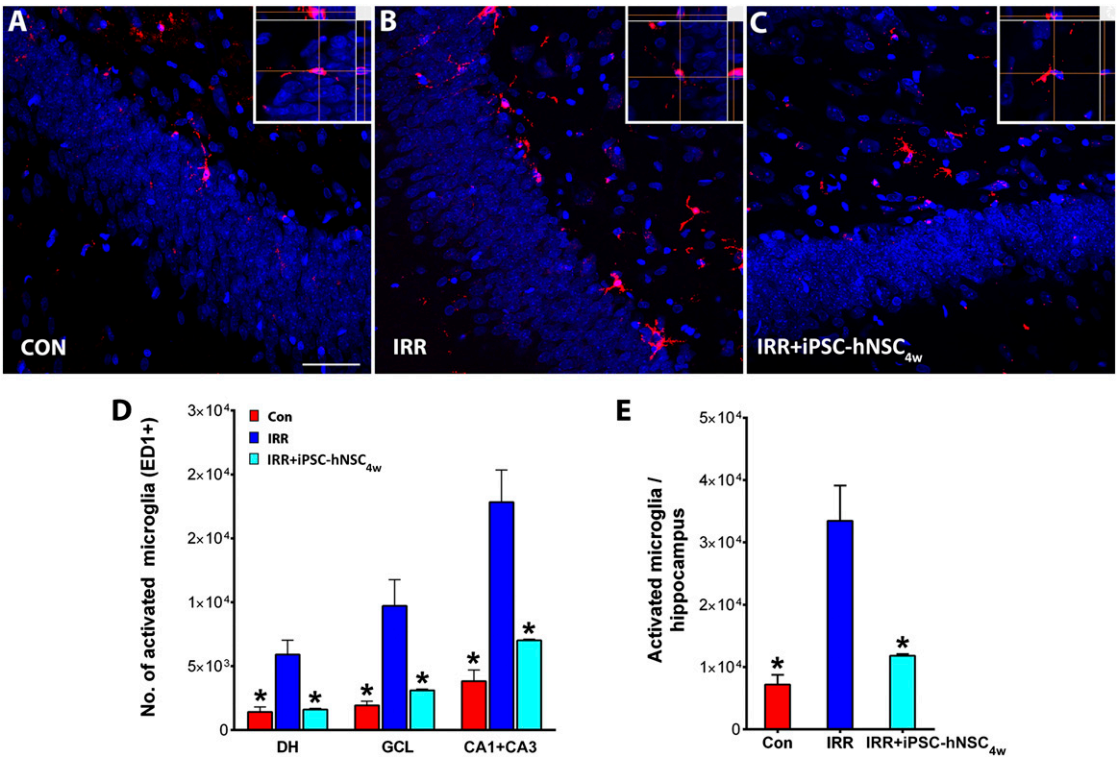

Figure 5. Transplantation of iPSC-hNSCs attenuated radiation-induced neuroinflammation. Immunofluorescence staining for activated microglia (red, ED-1+; blue, nuclear counterstain) in the hippocampus of CON, IRR, and IRR+iPSC$_{4w}$ groups **(A–C)**. At ~2.5 months after irradiation, the IRR group showed elevated microglia compared with the CON group in the DH, the GCL, and CA1+CA3 subfields **(D)** and throughout the hippocampus **(E)**. Intrahippocampal transplantation of iPSC-hNSCs at 4 weeks after irradiation (IRR+iPSC$_{4w}$) significantly reduced ED-1+ microglia in the host hippocampus including each subfield in which ED-1+ was analyzed (DH, GCL, and CA1+CA3) **(C–E)**. For each panel, insets represent orthogonal reconstructions of confocal *z*-stacks. ∗, $p < .05$ compared with IRR group. Scale bars = 50 μm **(A–C)**. Abbreviations: CON, nonirradiated sham-surgery group; DH, dentate hilus; GCL, granule cell layer; hNSC, human neural stem cell; iPSC, induced pluripotent stem cell; IRR, 10-Gy irradiated.

experimental conditions imposed on animal cohorts did not affect freezing behavior during the cue test phase, indicating intact acquisition and memory for the conditioned tone stimulus, a response shown to rely on intact amygdala function [18]. Consistent with the NPR decrements found, the specific deficits observed in contextual fear memory suggest that irradiation selectively disrupts hippocampal function, which corroborates much of our past data [5] and the known role of irradiation to inhibit hippocampal neurogenesis [17, 18]. A more limited series of studies conducted using normal human fibroblasts transplanted 2 days following cranial irradiation did not reveal any beneficial cognitive effects on hippocampal-dependent contextual fear memory (supplemental online Fig. 1). Although these data most likely reflect the absence of surviving engrafted fibroblasts at this time, they point to the benefits of using stem cells in these and similar types of approaches.

The appeal of stem cell therapy to treat virtually any ailment has stimulated an impressive array of research efforts into a wide variety of disorders [19–21]. The use of bone marrow transplantation following ablative radiotherapy demonstrates the successful application of stem cells to restore the hematopoietic system for the treatment of leukemia and lymphoma [22]. More recent preclinical and clinical studies have extended stem cell-based approaches to successfully treat a variety of normal tissueside effects resulting from radiation exposure (for review, see [23]). These studies have shown promise to treat radiation-induced hyposalivation (xerostomia) [24, 25], osteoradionecrosis [26], fibronecrosis of the skin [27], liver disease [28], proctitis [29–34], and cognitive dysfunction [5–7]. Despite the negative results obtained with engrafted human fibroblasts and the fact that current studies have used hNSCs derived from iPSCs, we cannot formally rule out the possibility that other nonstem or non-neural stem cells could impart beneficial effects to the irradiated brain. Nonetheless, the current work represents proof-of-principle studies, and although much work remains, ongoing research continues to show the promise of using stem cells to reduce the normal tissue complications associated with the radiotherapeutic management of cancer.

Examination of grafted iPSC-derived hNSCs revealed their presence throughout the septotemporal axis of the hippocampus in sufficient yield to significantly ameliorate cognitive dysfunction 1 month after irradiation and stem cell grafting. We focused our immunohistochemical assessments on the IRR+iPSC$_{4w}$ cohort because that time period provided the most significant improvements in cognition and because we have significant data at the earlier (2-day) postirradiation transplantation time. The vast majority of grafted cells (Ku80^{+}) found ventral to CA1 (Fig. 3) adopted neuronal phenotypes (DCX, Tuj1, or NeuN) (Fig. 4). Quantification of differentiated phenotypes confirmed that three of four dual-labeled Ku80^{+} engrafted cells committed to neuronal rather than astroglial cell fates (Fig. 4). Grafted cells positive for either immature or mature neuronal or astroglial markers did not exhibit any

overt morphologic abnormalities, and their presence did not cause any apparent disruption to the subtle architecture of the hippocampus. Moreover, the relative absence of proliferative and/or multipotent phenotypes (i.e., nestin$^+$ and Ki-67$^+$ cells) was consistent with the absence of teratoma formation, although longer term studies would be required to more conclusively rule out this possibility. Current results indicate that the levels of surviving grafted cells were sufficient to elicit functionally significant improvements in cognition following head-only irradiation.

Stem cell therapies for a variety of disorders have invariably identified the importance of trophic support provided to the injured host tissue [35, 36]. Longer term benefits ascribed to transplantation are generally considered not to result from cell replacement because graft survival and functional replacement of cells lost or damaged by a particular insult are difficult to realize in practice. Although the mechanisms underlying the beneficial effects of stem cell transplantation are certain to be complex and multifaceted, suppression of innate immunity in the brain may well attenuate persistent neuroinflammation and serve to dampen the immunological footprint of irradiation in the CNS. Radiation was found to elicit a marked and significant rise in activated microglia throughout the different subregions of the hippocampus; however, stem cell grafting was found to reduce this neuroinflammation to below background levels (Fig. 5). Precisely how grafted cells orchestrate reduced microglial activation in the irradiated brain is unclear, but their capability to moderate chemokine signaling through paracrine interactions with neighboring astrocytes (or other cell types) may suppress neuroinflammation to promote recovery of the brain [37–40]. Regardless of the mechanism, the presence of iPSC-derived grafted cells clearly reduces the levels of activated microglia in the irradiated brain, and this effect may contribute to overall or selected improvements in cognition.

Conclusion

With aging, the biochemical and structural complexity of the CNS undergoes a variety of reactive and degenerative processes. The onset or severity of these processes can be accelerated by disease, injury, genetic mutations, and exogenous insults such as irradiation. Although stem cell therapy will not likely obviate this progression, for cancer survivors and others forced to manage neurocognitive sequelae, stem cells may provide practical relief and a chance for improved quality of life. Given the absence of efficacious treatment options for the devastating side effects of cranial radiotherapy, stem cell therapy may provide a viable solution for this long-term mental health problem afflicting a growing number of cancer survivors.

Acknowledgments

This work was supported by National Institutes of Health, National Institute of Neurological Disorders and Stroke Grant R01-NS074388 (C.L.L.). We thank Dr. Martin Marsala, Dr. Cassiano Carromeu, and Dr. Alysson Muotri (University of California San Diego) for the induced pluripotent stem cell-derived human neural stem cells. We also thank Dr. Eugene Elmore for the growth of the IMR-90 cells used in this study.

Author Contributions

M.M.A.: conception and design, collection and assembly of data, data analysis and interpretation, manuscript writing; V.M.: collection and assembly of data, data analysis; L.-A.C.: data analysis and interpretation; L.R.: collection and assembly of data; J.S.: provision of study material; V.K.P.: collection and assembly of data, data analysis and interpretation, manuscript writing; C.L.L.: conception and design, data interpretation, manuscript writing, financial support, administrative support, final approval of manuscript.

Disclosure of Potential Conflicts of Interest

L.-A.C. is a compensated employee of Allergan, Inc. The other authors indicated no potential conflicts of interest.

References

1 Butler JM, Rapp SR, Shaw EG. Managing the cognitive effects of brain tumor radiation therapy. Curr Treat Options Oncol 2006;7:517–523.

2 Meyers CA. Neurocognitive dysfunction in cancer patients. Oncology (Williston Park) 2000 14:75–79; discussion 79, 81-82, 85.

3 Douw L, Klein M, Fagel SS et al. Cognitive and radiological effects of radiotherapy in patients with low-grade glioma: Long-term follow-up. Lancet Neurol 2009;8:810–818.

4 Meyers CA, Brown PD. Role and relevance of neurocognitive assessment in clinical trials of patients with CNS tumors. J Clin Oncol 2006;24:1305–1309.

5 Acharya MM, Christie LA, Hazel TG et al. Transplantation of human fetal-derived neural stem cells improves cognitive function following cranial irradiation. Cell Transplant 2014;23:1255–1266.

6 Acharya MM, Christie LA, Lan ML et al. Rescue of radiation-induced cognitive impairment through cranial transplantation of human embryonic stem cells. Proc Natl Acad Sci USA 2009;106:19150–19155.

7 Acharya MM, Christie LA, Lan ML et al. Human neural stem cell transplantation ameliorates radiation-induced cognitive dysfunction. Cancer Res 2011;71:4834–4845.

8 Christie LA, Acharya MM, Limoli CL. Quantifying cognitive decrements caused by cranial radiotherapy. J Vis Exp 2011;(56):pii:3108.

9 Parihar VK, Acharya MM, Roa DE et al. Defining functional changes in the brain caused by targeted stereotaxic radiosurgery. Transl Cancer Res 2014;3:124–137.

10 Parihar VK, Limoli CL. Cranial irradiation compromises neuronal architecture in the hippocampus. Proc Natl Acad Sci USA 2013;110:12822–12827.

11 Parihar VK, Pasha J, Tran KK et al. Persistent changes in neuronal structure and synaptic plasticity caused by proton irradiation. Brain Struct Funct 2014 [Epub ahead of print].

12 Piltti KM, Salazar DL, Uchida N et al. Safety of human neural stem cell transplantation in chronic spinal cord injury. Stem Cells Translational Medicine 2013;2:961–974.

13 Marchetto MC, Carromeu C, Acab A et al. A model for neural development and treatment of Rett syndrome using human induced pluripotent stem cells. Cell 2010;143:527–539.

14 Christie LA, Acharya MM, Parihar VK et al. Impaired cognitive function and hippocampal neurogenesis following cancer chemotherapy. Clin Cancer Res 2012;18:1954–1965.

15 Kiskinis E, Eggan K. Progress toward the clinical application of patient-specific pluripotent stem cells. J Clin Invest 2010;120:51–59.

16 Marchetto MC, Winner B, Gage FH. Pluripotent stem cells in neurodegenerative and neurodevelopmental diseases. Hum Mol Genet 2010;19:R71–R76.

17 Winocur G, Wojtowicz JM, Sekeres M et al. Inhibition of neurogenesis interferes with hippocampus-dependent memory function. Hippocampus 2006;16:296–304.

18 Phillips RG, LeDoux JE. Differential contribution of amygdala and hippocampus to cued and contextual fear conditioning. Behav Neurosci 1992;106:274–285.

19 Blurton-Jones M, Kitazawa M, Martinez-Coria H et al. Neural stem cells improve cognition via BDNF in a transgenic model of Alzheimer disease. Proc Natl Acad Sci USA 2009;106:13594–13599.

20 Boison D. Engineered adenosine-releasing cells for epilepsy therapy: Human mesenchymal stem cells and human embryonic

stem cells. Neurotherapeutics 2009;6:278–283.

21 Riess P, Molcanyi M, Bentz K et al. Embryonic stem cell transplantation after experimental traumatic brain injury dramatically improves neurological outcome, but may cause tumors. J Neurotrauma 2007;24:216–225.

22 Greenberger JS, Epperly M. Bone marrow-derived stem cells and radiation response. Semin Radiat Oncol 2009;19:133–139.

23 Benderitter M, Caviggioli F, Chapel A et al. Stem cell therapies for the treatment of radiation-induced normal tissue side effects. Antioxid Redox Signal 2014;21:338–355.

24 Lombaert IM, Brunsting JF, Wierenga PK et al. Rescue of salivary gland function after stem cell transplantation in irradiated glands. PLoS One 2008;3:e2063.

25 Nanduri LS, Maimets M, Pringle SA et al. Regeneration of irradiated salivary glands with stem cell marker expressing cells. Radiother Oncol 2011;99:367–372.

26 Espitalier F, Vinatier C, Lerouxel E et al. A comparison between bone reconstruction following the use of mesenchymal stem cells and total bone marrow in association with calcium phosphate scaffold in irradiated bone. Biomaterials 2009;30:763–769.

27 Ebrahimian TG, Pouzoulet F, Squiban C et al. Cell therapy based on adipose tissue-derived stromal cells promotes physiological and pathological wound healing. Arterioscler Thromb Vasc Biol 2009;29:503–510.

28 Guha C, Sharma A, Gupta S et al. Amelioration of radiation-induced liver damage in partially hepatectomized rats by hepatocyte transplantation. Cancer Res 1999;59:5871–5874.

29 Kudo K, Liu Y, Takahashi K et al. Transplantation of mesenchymal stem cells to prevent radiation-induced intestinal injury in mice. J Radiat Res (Tokyo) 2010;51:73–79.

30 Lorenzi B, Pessina F, Lorenzoni P et al. Treatment of experimental injury of anal sphincters with primary surgical repair and injection of bone marrow-derived mesenchymal stem cells. Dis Colon Rectum 2008;51:411–420.

31 Saha S, Bhanja P, Kabarriti R et al. Bone marrow stromal cell transplantation mitigates radiation-induced gastrointestinal syndrome in mice. PLoS One 2011;6:e24072.

32 Sémont A, François S, Mouiseddine M et al. Mesenchymal stem cells increase self-renewal of small intestinal epithelium and accelerate structural recovery after radiation injury. Adv Exp Med Biol 2006;585:19–30.

33 Voswinkel J, Francois S, Simon JM et al. Use of mesenchymal stem cells (MSC) in chronic inflammatory fistulizing and fibrotic diseases: A comprehensive review. Clin Rev Allergy Immunol 2013;45:180–192.

34 Zhang J, Gong JF, Zhang W et al. Effects of transplanted bone marrow mesenchymal stem cells on the irradiated intestine of mice. J Biomed Sci 2008;15:585–594.

35 Chen WW, Blurton-Jones M. Concise review: Can stem cells be used to treat or model Alzheimer's disease? STEM CELLS 2012;30:2612–2618.

36 Martínez-Morales PL, Revilla A, Ocaña I et al. Progress in stem cell therapy for major human neurological disorders. Stem Cell Rev 2013;9:685–699.

37 Belarbi K, Jopson T, Arellano C et al. CCR2 deficiency prevents neuronal dysfunction and cognitive impairments induced by cranial irradiation. Cancer Res 2013;73:1201–1210.

38 Li Y, Liu Z, Xin H et al. The role of astrocytes in mediating exogenous cell-based restorative therapy for stroke. Glia 2014;62:1–16.

39 Xin H, Li Y, Buller B et al. Exosome-mediated transfer of miR-133b from multipotent mesenchymal stromal cells to neural cells contributes to neurite outgrowth. STEM CELLS 2012;30:1556–1564.

40 Xin H, Li Y, Liu Z et al. MiR-133b promotes neural plasticity and functional recovery after treatment of stroke with multipotent mesenchymal stromal cells in rats via transfer of exosome-enriched extracellular particles. STEM CELLS 2013;31:2737–2746.

See www.StemCellsTM.com for supporting information available online.

